



## Research article

## Automated identification of toxigenic cyanobacterial genera for water quality control purposes

Iman Kianian<sup>a</sup>, MohammadSadeq Mottaqi<sup>b</sup>, Fatemeh Mohammadipanah<sup>c,\*\*</sup>, Hedieh Sajedi<sup>a,\*</sup><sup>a</sup> Department of Computer Science, School of Mathematics, Statistics and Computer Science, College of Science, University of Tehran, Tehran, Iran<sup>b</sup> The Graduate Center, The City University of New York, New York, NY, United States<sup>c</sup> Department of Microbial Biotechnology, School of Biology and Center of Excellence in Phylogeny of Living Organisms, College of Science, University of Tehran, 14155-6455, Tehran, Iran

## ARTICLE INFO

## Keywords:

Image recognition  
Toxic cyanobacteria genera  
Cyanobacteria classification  
MobileNet  
VGG  
Water quality monitoring

## ABSTRACT

Cyanobacteria are the dominating microorganisms in aquatic environments, posing significant risks to public health due to toxin production in drinking water reservoirs. Traditional water quality assessments for abundance of the toxigenic genera in water samples are both time-consuming and error-prone, highlighting the urgent need for a fast and accurate automated approach. This study addresses this gap by introducing a novel public dataset, TCB-DS (Toxigenic Cyanobacteria Dataset), comprising 2593 microscopic images of 10 toxigenic cyanobacterial genera and subsequently, an automated system to identify these genera which can be divided into two parts. Initially, a feature extractor Convolutional Neural Network (CNN) model was employed, with MobileNet emerging as the optimal choice after comparing it with various other popular architectures such as MobileNetV2, VGG, etc. Secondly, to perform classification algorithms on the extracted features of the first section, multiple approaches were tested and the experimental results indicate that a Fully Connected Neural Network (FCNN) had the optimal performance with weighted accuracy and f1-score of 94.79% and 94.91%, respectively. The highest macro accuracy and f1-score were 90.17% and 87.64% which were acquired using MobileNetV2 as the feature extractor and FCNN as the classifier. These results demonstrate that the proposed approach can be employed as an automated screening tool for identifying toxigenic Cyanobacteria with practical implications for water quality control replacing the traditional estimation given by the lab operator following microscopic observations. The dataset and code of this paper are publicly available at <https://github.com/iman2693/CTCB>.

## 1. Introduction

Cyanobacteria are known for their crucial role as primary producers and oxygen generators in aquatic ecosystems, making them a dominant group of microorganisms in euphotic environments. However, they biosynthesize secondary metabolites called cyanotoxins with carcinogenic effects on the liver and nervous system of humans and animals. Global warming increases concerns about the proliferation of Cyanobacteria, causing hazardous blooms that negatively impact drinking water quality and consequently plant and animal health (Vaughan et al., 2022; Moreira et al., 2022).

Various pollutants, including pathogenic microorganisms and their byproducts, such as toxins generated by Cyanobacteria, geogenic

compounds such as fluoride, iodine, and cadmium, as well as factory-made and agricultural contaminants, such as poly-fluoroalkyl substances and fertilizers, have all been identified as health concerns in freshwater (Prüss-Ustün et al., 2019). As a result, water safety and quality management strategies monitor and quantify the above-mentioned chemical and biological agents. Thus, if the cell number of toxigenic Cyanobacteria in drinking water supplies is not properly managed, the public may be at risk of developing neurological or cancer diseases. Regulations concerning the monitoring of hazardous Cyanobacteria have yet to be fully implemented in most nations' quality controls as most water utilities have difficulty initiating modern, efficient water quality management operations (Bernard et al., 2007; World Health, 2017). To address this issue, the U.S. Environmental Protection

\* Corresponding author.

\*\* Corresponding author.

E-mail addresses: [kianian@ut.ac.ir](mailto:kianian@ut.ac.ir) (I. Kianian), [mmottaqi@gradcenter.cuny.edu](mailto:mmottaqi@gradcenter.cuny.edu) (M. Mottaqi), [fmohammadipanah@ut.ac.ir](mailto:fmohammadipanah@ut.ac.ir) (F. Mohammadipanah), [hhsajedi@ut.ac.ir](mailto:hhsajedi@ut.ac.ir) (H. Sajedi).<https://doi.org/10.1016/j.jenvman.2024.121274>

Received 6 September 2023; Received in revised form 27 April 2024; Accepted 26 May 2024

Available online 4 June 2024

0301-4797/© 2024 Elsevier Ltd. All rights reserved, including those for text and data mining, AI training, and similar technologies.

Agency (EPA) recently published a handbook recommending a variety of rapid tests and laboratory techniques to find and recognize Cyanobacteria and their toxins in water samples, including Liquid chromatography–mass spectrometry (LC-MS), Phosphatase-inhibition assays (PIAs), Enzyme immunoassay (EIA), and Quantitative polymerase chain reaction (qPCR) (Agency, 2022).

Although detoxification techniques, including the reduction of cyanotoxins to an acceptable concentration, can be employed to reduce the levels of cyanotoxins, safe neutralization methods are still not available. There are multiple methods to detect or monitor the trend of toxigenic cyanobacterial abundance in water samples, including cell detection (Jin et al., 2018), biosensors (Thakur et al., 2018), PCR-based (Cooley et al., 2018), and metagenomics (Roy et al., 2018). Nevertheless, microscopy followed by image analysis is a basic and universal type of screening approach, as these toxin analysis techniques demand sophisticated instruments, experts, and cyanotoxin reference compounds.

While numerous studies have proposed innovative methods for cell enumeration of bacteria in water samples, the detection and enumeration of specific groups such as Cyanobacteria remain a significant challenge in Cyanobacteria monitoring operations as most members of this group are filamentous rather than single cell. Manual assessment of water samples for toxigenic Cyanobacteria on microscope slides by skilled professionals is labor-intensive and error-prone (Bernard et al., 2007). Therefore, the automation of the visual interpretation practices as a part of the operation procedures can reduce the challenges and false positive or negative recognitions.

Although there are several studies and publicly available datasets in the field of bacteria classification, limited studies have been done on Cyanobacteria specifically. Among the presented studies, some works used aerial imagery such as satellite images to quantify cyanobacterial groups in lakes or ponds (Bunyon et al., 2023; Kim et al., 2023) and there is no report focusing on the identification of different types of Cyanobacteria using microscopic images. The only attempt for this purpose has been on other prevalent photosynthetic microorganisms called microalgae. Furthermore, there are currently no publicly available datasets in this specific field.

This study has two phases to cover these existing gaps. Firstly, we conducted a new publicly available dataset called TCB-DS comprising light microscopic images of the most toxin-producing genera of Cyanobacteria (Table S1). This dataset offers a valuable resource for the scientific community, facilitating the development of potential future more accurate automated models. In the second phase, to show the reliability and validation of this dataset, we utilized Convolutional CNN to perform an automated detection of the most highly toxigenic cyanobacterial genera. Our classification and analysis involve selecting microscopic images of 10 genera that are capable of producing more than two types of cyanotoxins. Given the limited size of the available training set, pre-trained CNN models were preferred over building and training a model from scratch.

The following summarizes the main contributions of this paper.

- A comprehensive study of the related literature including previous research on machine learning for Cyanobacteria analysis.
- Introduction of a new publicly available dataset named TCB-DS comprising toxic cyanobacterial microscopic images.
- A novel method for identifying cyanobacterial genera, using convolutional neural networks, that is robust to dataset flaws and improves accuracy in detecting toxigenic genera.
- Demonstrations of practical applications of the system in real-world scenarios, highlighting its capability to improve water quality monitoring in the future.

The subsequent sections of this paper are structured as follows: Section II reviews the related work on image analysis of Cyanobacteria and other types of algae. Section III provides a detailed description of the TCB-DS and the proposed model for classifying images of the dataset.

Section IV presents the experimental setup, results, and analysis. Section V discusses the limitations and future work of our method and the dataset. Section VI concludes the paper.

## 2. Related works

In this section, some related works in the field of autonomous identification of cyanobacterial genera have been reviewed. Initially, our focus will be on exploring literature specifically related to Cyanobacteria. Additionally, given the limited number of studies in this particular area, our review also encompasses works related to other bacterial groups.

## 3. Cyanobacteria

In the realm of Cyanobacteria, many studies have been conducted in recent years, but there are a limited number of studies that focused on utilizing AI systems to identify Cyanobacteria using their cellular features. The available studies which used AI systems for these purposes can be divided into two categories. In the first category, which is more related to our aim, microscopic images of cyanobacterial genera are the main focus of the study, and in the second one, aerial images such as satellite images are analyzed. In the following section, we will discuss some recent works in both areas.

## 4. Microscopic images

The first group of papers related to the identification of Cyanobacteria focuses on the microscopic modality. As the first example, Baek et al. (2020) presented an approach to the classification and quantification of cyanobacterial genera including 5 different types *Microcystis aeruginosa*, *Microcystis wesenbergii*, *Oscillatoria*, *Aphanizomenon*, and *Dolichospermum*. The authors employed deep a fast regional convolutional neural network (R-CNN) and a CNN, to achieve their objectives. Although they achieved valuable results, their dataset is not publicly available for future investigation and comparisons.

In another work, Sonmez et al. (2022) proposed a method to differentiate two type of photosynthetic microorganisms: Cyanobacteria and Chlorophyta. Images captured using an inverted microscope were classified using two different methods. The first method involved classification performed with seven different CNN models. The second method employs the Support Vector Machine (SVM) after the AlexNet model. The outcome of this work was differentiating the Cyanobacteria from Chlorophyta. However, they did not provide any publicly available dataset for further research.

In another investigation, Gaur et al. (2022) applied AlexNet and VGG16 for feature extraction of microscopic images of ten common cyanobacterial genera of the blooms. They performed fusion on the last fully connected layers of these models. With these features, they proposed an Alex-VGG convolution fusion network (CFN) for classification purposes. The 10 cyanobacterial genera which they included in their dataset were *Anabaena constricta*, *Chroococcus turgidus*, *Kamptomena* sp., *Lyngbya* sp., *Microcystis aeruginosa*, *Nostoc punctiforme*, *Oscillatoria formosa*, *Phormidium tenue*, *Phormidium ambiguum*, *Scytonema coactile* which is a good diversity of existing harmful cyanobacterial genera. They also did not make their dataset publicly available, and as a result, other investigations cannot use their dataset.

A notable study by Kraft et al. (2021) applied Imaging-in-Flow Cytometry (IFCB) to capture high-frequency images of bloom-forming filamentous Cyanobacteria, achieving acceptable results in real-time monitoring of these organisms in the Baltic Sea. Their research demonstrated significant improvements in detection accuracy and processing speed, highlighting the IFCB's capability to identify various cyanobacterial genera with an identification accuracy surpassing 90%.

It is crucial to note that genera such as *Raphidiopsis* and *Cylindrospermopsis* are scarcely represented in existing datasets. This

underrepresentation is problematic as these genera can produce toxins that pose health risks, yet their infrequent blooms make them less likely to be captured in routine sampling. Addressing this gap is essential for developing AI models that can effectively recognize and respond to these rare but significant threats.

In conclusion, the availability of standardized datasets plays a crucial role in advancing scientific research by allowing researchers to benchmark their methods against existing approaches and facilitating the development of more accurate and robust algorithms. However, the absence of publicly accessible datasets in the field of cyanobacteria identification poses a significant challenge to researchers looking to build upon existing work or develop new methodologies.

## 5. Satellite image analysis for estimation of cyanobacterial load

As mentioned in previous sections, in the second approach to cyanobacteria image analysis, aerial images have been used for modeling. Most of these datasets used satellite modality. For example, [Pyo et al. \(2020\)](#) proposed an approach using CNN for predicting bloom formation by Cyanobacteria. They generated synthetic spatio-temporal water quality data using a 3D water quality model and used this data to train the CNN. In another similar work [Zhang et al. \(2023\)](#) presented a comparative study of two machine learning models - the least absolute shrinkage and selection operator (LASSO) regression model and the random forest (RF) model - for predicting cyanobacterial abundance in aquaculture ponds. Such models, based on the intensity of their pigment absorbance in satellite images, have applications in comparing the load of Cyanobacteria among different water bodies ([Tavakoli et al.](#)) or at different times. Although there are other valuable works in this area, we overlook similar works due to their dissimilarity to our work in terms of image modality.

## 6. Other bacteria types

As mentioned, due to the limited research conducted on microscopic images of Cyanobacteria, we have opted to include some studies from related fields to analyze and draw broader conclusions. As the first example, because of diverse approaches in this field, we separated this part into three different sub categories including traditional approaches, CNN-based approaches, and Transfer-learning approaches.

## 7. Traditional approaches

One of the earliest efforts to automate bacterial genera classification was proposed by [Liu et al. \(2001\)](#). They developed an automatic computer-aided system, called "CMEIAS" (an image analysis program) which used morphological characteristics and a KNN classifier to classify bacterial species' morphotypes. However, in the past years, other traditional methods for the automated detection of bacterial species have been proposed. [Promdaen et al. \(2014\)](#) employed several approaches for segmenting cyanobacterial images from an image background, computing texture descriptors from a blurry texture object, and Sequential Minimal Optimization was used as a classifier. [Men et al. \(2008\)](#) presented a SVM model for classifying heterotrophic bacteria colonies that were somewhat more advanced than earlier approaches. In those years, Neural Networks (NN) did not have much power and were rarely used. After some years, artificial neural networks and especially deep learning approaches have gained popularity because they outperform more conventional ML techniques in terms of learning capacity and generalization error. With the introduction of neural networks, they quickly replaced older methods for all learning tasks and were also used to solve the issue of autonomous classification of bacterial species. For instance Study ([Xiaojuan and Cunshe, 2009](#)) is one of the earliest uses of simple neural networks. A three-layered Back Propagation Neural Network (BPNN) was recommended by Xiaojuan et al. ([Xiaojuan and Cunshe, 2009](#)) for the image recognition of wastewater bacterial species.

Feature extraction of the input images was performed with some traditional approaches, PCA performed for dimensionality reduction and BPNN was used for doing just classification as an alternative to classical classification algorithms like SVM. The majority of classic approaches for automated bacterium classification are built to handle one-dimensional vector information is one of their disadvantages. Hence, before using traditional image recognition techniques, they should first extend the image matrix to a one-dimensional vector or extract features from images that would lose adjacent information from images and overlook some crucial aspects. However, some studies do not employ the end-to-end approaches used by deep models. Instead, they attempt to capture spatial features without utilizing any deep architecture, relying on certain morphological operators. As an example, Deglint and coworkers ([Deglint et al., 2019](#)) proposed a method that leverages feed-forward neural networks and fluorescence-based spectral-morphological features for the automated recognition of six diverse types of algae.

## 8. Deep architectures

In order to deal with the mentioned problem of traditional approaches, some other newer methods based on deep neural networks such as CNN have been proposed and used. As one of the first applications of CNNs in the automatic classification and identification of bacterial species, Lopez et al. ([Yadini Pérez López et al., 2017](#)) presented an automatic identification of mycobacterium tuberculosis (MT) using CNN approaches. Before training the model, they augmented the source dataset to obtain 9770 images. In another work, Park and colleagues ([Park et al., 2019](#)) employed neural architecture search to discover the optimal CNN model for classifying eight algal genera in watersheds with algal blooms. Their technique effectively classified the algal genera, resulting in an F1-score of 0.95 for all eight genera. Some other deep approaches presented in the recent years. Pardeshi et al. ([Pardeshi and Deshmukh, 2023b](#)) also worked on another similar subject which was the classification of 17 microscopic algae including *Achnanthesidium*, *Nostoc*, etc. In this they used a compact CNN that requires fewer computational resources while maintaining high accuracy in microalgae species identification. As another example, Otalora et al. ([Otalora et al., 2023](#)) presented an innovative approach to the characterization of microalgae cultures using a AlexNet-based model. They developed a model that leverages data acquired from a device called FlowCam which captures images of the cells detected in a culture sample, which are then used as inputs by the model.

In the recent years with emerging transformers in the field of machine vision, different studies used this neural network as an alternative of CNN models. In fact, these networks show their potential power in different fields like image classification or segmentation. The applications of transformers in the field of bacteria classification have just begun. As one of the first tries, In a most recent approaches, [Lu et al. \(2024\)](#) presented a highly compatible and cost-effective solution for bacterial species detection that combines hyperspectral microscopic imaging (HMI) with a Transformer network for the classification of infectious bacteria.

## 9. Transfer-learning approaches

As typical deep models have lots of trainable parameters and due to the massive size of 2-dimensional images with 3 channels (RGB) and a small number of data, training these models nicely from scratch is almost impractical. As we mentioned before, for the purpose of carrying off this problem, transfer learning approaches were proposed. Using the transfer learning methods reduces the need for a large amount of data and therefore performed better for modeling most bacterial image datasets. Studies ([Khalifa et al., 2019](#); [Nasip and Zengin, 2018](#); [Shaily and Kala, 2020](#); [Talo, 2019](#); [M. F. Wahid et al., 2018](#); [Zieliński et al., 2017](#); [Pardeshi and Deshmukh, 2023a](#)) used transfer-learning approach

to deal with the described problem. Wahid et al. (M. F. Wahid et al., 2018) proposed a transfer-learning based approach for the classification of bacterial microscopic images. They used the transfer-learning approach to deal with the described problem.

A dataset called DIBAS (Digital Images of Bacteria Species dataset), which contains 660 photos for 33 different bacterial species, was introduced by Bartosz Zieliński et al. (2017) in 2017. Eventually, the DIBAS dataset evolved into a public and standard dataset for research on bacteria image analysis, and as a result, it has been utilized in numerous studies that will be discussed further. The authors also used the Fisher vector (FV), a combination of SVM and RF with some pre-trained CNN models such as AlexNet, VGG-M, and VGG-VD for purpose of automatic identification of different bacteria species in the DIBAS dataset. For the DIBAS dataset, several additional papers have attempted to improve classification performance, and the majority of them have utilized the transfer-learning strategy. Khalifa et al. (2019) first applied some data augmentation techniques to increase the size of the DIBAS dataset and then used a fine-tuned pre-trained AlexNet to classify the DIBAS images.

The other attempt to achieve better accuracy by Nasip et al. (Nasip and Zengin, 2018) was not successful. Based on the presented VGG model by Karen Simonyan and Andrew Zisserman (Simonyan and Zisserman, 2014), Nasip et al. (Nasip and Zengin, 2018) after using data augmentation, performed pre-trained AlexNet and VGG-16 but the accuracy did not increase with compare to Khalifa's method. It could be proven by Occam's Razor rule that Khalifa's method is better than Nasip's. Nasip's method used much more parameters and training data than Khalifa's, but the achieved accuracies in these two studies are the same (98.2%). For more information, VGG-16 has about 138 million parameters which are too high with compare to AlexNet which has about 60 million parameters. In the continuation of methods based on transfer learning Muhammed Talo (2019) proposed a CNN pre-trained model to classify the bacteria species in the DIBAS dataset. In this study, a pre-trained CNN architecture known as ResNet-50 was used. The fully connected layers at the end of the ResNet-50 were removed and replaced with a new fully connected layer to categorize bacterial species with better accuracy with compare to previous methods. Compared to VGG-16 and AlexNet (two previous proposed studies), the employed model (ResNet-50) is deeper and has more parameters, yet it is still valuable for use due to its higher accuracy.

Similar to Talo's paper (Talo, 2019), Shaily et al. (Shaily and Kala, 2020) also used pre-trained ResNet-50 with the difference that only 20 out of 33 species of DIBAS were selected for classification. An accuracy of 99.90% was obtained. Although this value is higher than the previous accuracies, this cannot be compared with the previous studies because some of the classes in the DIBAS dataset were omitted.

As seen, many studies have used methods based on the transfer learning concept to model image data of bacteria species. The majority of those studies focus on the classification of the general bacteria species not only Cyanobacteria. There have been existing other research that work especially on the classification of different types of Cyanobacteria using microscopic images as input. For instance, Jungsu Park et al. (2019) used a dataset from 1158 algal images from 8 different species to train several models which are based on CNN architectures. Some of these models trained using augmented training data which contains 5790 images and augmented from the original images by mirroring, rotating, and top-down flipping. The best developed CNN model which was a CNN model extracted from a neural architecture search (NAS), classified the algal genus with an F1-score of 0.95 for the eight genera.

Using pre-trained networks is not just limited to previous years. Nowadays it is used to cover the dataset size limitation. In a recent study, Pardeshi et al. (Pardeshi and Deshmukh, 2023a) aimed to automate the laborious task of manually classifying Desmids which are a group of green algae that are often used as indicators of water quality in aquatic ecosystems. They employed transfer learning and CNNs like ViTnet, Squiznet, and AlexNet to achieve this. In another recent research in this field, Figueroa et al. (2024) addressed the critical issue of water quality,

which can be negatively affected by certain toxic phytoplankton genera. The dataset comprises 293 color microscopic images, each containing multiple phytoplankton specimens of varying species. The images, with a resolution of 0.33  $\mu\text{m}$  per pixel, were captured using an optical microscope at a magnification of  $10\times$ . Water samples were collected from Lake Doñiños (Ferrol, Galicia, Spain) at different depths and times of the year to represent the lake's biomass under varying conditions. The authors proposed using deep learning techniques to detect and recognize phytoplankton specimens in multi-specimen microscopy images. They used two object detectors Faster R-CNN and RetinaNet which were pre-trained on the COCO dataset. Also, for the classifier, the used ResNet50 pre-trained on the ImageNet. The positive aspect of this research is that the dataset used is publicly available, which can enhance reproducibility and encourage new ideas in the field.

In summary, traditional methods, such as morphological characteristics and KNN classifiers, have been used for bacterial species classification, while other approaches have focused on segmenting images and using texture descriptors and sequential minimal optimization for classification. Traditional approaches are not suitable for handling picture data, as Deep Neural Networks (DNNs) outperform them in terms of learning capacity and generalization error. The disadvantage of the classical approaches for image classification is that they are not suitable for receiving picture data and are built to handle one-dimensional vector information. Thus, before using traditional image recognition techniques, the image matrix should be extended to a one-dimensional vector or extract features from images that would lose adjacent information from images and overlook some crucial aspects. To deal with this problem, more recent methods based on DNNs such as CNN have been proposed and used. Recently, deep learning techniques, such as CNNs, have been introduced to solve the issue of autonomous classification of bacterial species. Transfer learning-based approaches have been proposed to overcome the challenge of having a large number of trainable parameters for CNN models, and different pre-trained CNN architectures, such as InceptionV1 and ResNet-50, have been fine-tuned for feature extraction tasks. These approaches have been used to classify bacteria images to different species with high accuracy, and several datasets, such as the Digital Images of Bacteria Species (DIBAS) dataset, have been established for works related to bacteria image analysis.

## 10. Methods and material

In this section, the methods used for the TCB-DS preparation and automated classification of Cyanobacteria are both presented in depth. Fig. 1 shows a summary of a high-level roadmap of the proposed method after data pre-processing. For classification purposes, we trained the developed models with microscopic images of 10 highly toxic cyanobacterial genera. These genera are the ones producing at least two different cyanotoxins. Due to diverse sources of gathered images mentioned in the method section, the inappropriate images were omitted and useable images were cropped manually which formed the proposed TCB-DS. After this step, some preprocessing such as padding, upsampling, downsampling, etc. Were used to prepare images for feeding the proposed method.

## 11. TCB-DS preparation

### 11.1. Selection of toxigenic cyanobacteria

There are at least 30 cyanobacteria genera producing at least one type of cyanotoxins. Out of the total toxigenic genera, 10 genera (*Anabaena*, *Aphanizomenon*, *Cylindrospermopsis*, *Dolichospermum*, *Microcystis*, *Nostoc*, *Oscillatoria*, *Phormidium*, *Planktothrix*, and *Raphidiopsis*), which often produce more than two types of toxins, were selected for subsequent analysis.



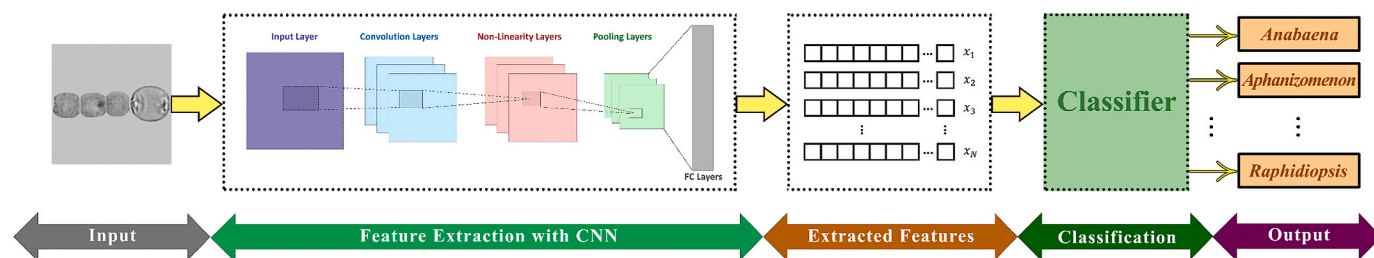


Fig. 1. The structure of the proposed method for automatic identification of the genera.

### 11.2. Collection of cyanobacterial images

To construct the dataset required for training our model to identify the toxigenic genera, microscopic pictures of the 10 chosen genera were derived from the databases listed in Table S2.

To construct the TCB-DS dataset required for training our model on identify the toxigenic genera, we meticulously sourced microscopic images of 10 chosen cyanobacterial genera from multiple reputable databases, as detailed in Table S2. For each image, we extracted crucial metadata including the imaging equipment used, typically high-resolution microscopes such as the Zeiss Axioskop and Olympus BX53, which are renowned for their precision in biological imaging. The scale of the images varied, but generally maintained a high enough resolution to clearly depict distinctive morphological features of the cyanobacteria, crucial for accurate classification. This diversity in imaging sources and scales ensured a robust dataset, capable of training an AI to recognize and classify a wide variety of cyanobacterial forms under different visual conditions.

### 11.3. Preparing the TCB-DS

Designing an autonomous image processing approach for the automatic segmentation of samples from photos was difficult since the sources of the collected images varied in terms of factors including contrast, resolution, size, lighting, having noise, and microscopic scale. Therefore, to form a dataset for automatic recognition of Cyanobacteria, the appropriate collected samples were cropped manually and the others were excluded. For some images, due to their same characteristics (size, magnification level, etc.), the useful patches of the original images were separated by running a script and then manually checked to make sure they were not meaningless. It should be mentioned that the intersections of manually cropped images are less than 10% in terms of spatial position. The TCB-DS dataset characteristics are formed in Table 1. Following the manual cropping described above, an 80:20 split was used to separate the training and test sets. Table 2 lists the number of samples in the training (before applying resampling) and test set per class. In the last step, separated images with variable sizes were saved in the train and test folder separately and the resulting dataset - named TCB-DS - is a

Table 1  
Main features of the proposed TCB-DS dataset.

Property	Value
Dataset Name	TCB-DS
Number of Images	2591 (train and test)
Image type	Microscopic
Image Dimensions	Variable (Minimum = $11 \times 41$ px, Maximum = $5184 \times 3456$ px, Mode = $150 \times 150$ px, Average = $165 \times 157$ px, Std = $102 \times 120$ px)
Image Format	.PNG
Magnification Level	$5 \mu\text{m}$ – $100 \mu\text{m}$
Color Profile	RGB
Source of Images	Table S2
Number of Classes/Labels	10

Table 2

Number of samples in the training and test set of TCB-DS per each genus and result of performing resampling.

Class labels	No. Of images in training set before resampling (Original Images)	No. Of images in training set after resampling	No. Of images in test set
<i>Anabaena</i>	268	267	56
<i>Aphanizomenon</i>	30	232	4
<i>Cylindrospermopsis</i>	23	220	3
<i>Dolichospermum</i>	130	384	33
<i>Microcystis</i>	895	459	235
<i>Nostoc</i>	237	236	73
<i>Oscillatoria</i>	157	310	32
<i>Phormidium</i>	224	222	61
<i>Planktothrix</i>	104	312	19
<i>Raphidiopsis</i>	5	210	2
<b>Total</b>	<b>2073</b>	<b>2852</b>	<b>518</b>

separated dataset.

## 12. Preprocessing of the TCB-DS

Due to manual cropping, there are images in the training and test sets of TCB-DS with different sizes which smallest one is of size  $11 \times 41$  and the largest one is of size  $5184 \times 3456$ . Therefore, all images in the TCB-DS – including the training and test sets – was resized to a size of  $150 \times 150$  by downscaling and upscaling. In order to upscale the images, all empty pixels were filled by a color collected by averaging the values of the RGB channels of pixels around each manually cropped image in TCB-DS as shown in Figure S1. Since different Cyanobacteria species are distinguished according to their shape, the color of the image is not needed to identify the type of Cyanobacteria and its appearance and shape are important (Mehdizadeh Allaf and Peerhossaini, 2022). Thus, after equalizing the size of the images to  $150 \times 150$ , all images were converted from 32-bit RGB to 8-bit grayscale. Following manual cropping and resizing, downsampling was performed for classes that have a large number of samples while for classes with fewer samples, upsampling has been used to make a balanced training set. A variety of methods was employed for upsampling, including transformation, flipping, rotation, etc. And the parameters of their augmentation are presented in Table 3. A probability was employed to choose each image for downsampling. This probability was shown in Eq. (1). The first two columns of Table 2 show that after applying upsampling and downsampling, an almost balanced training set was reached. A summary of

Table 3  
Image augmentation parameters.

Techniques	Limitations
Rotation (degree)	$-90^\circ/90^\circ$
Shift (pixel)	30 px
Zoom (percent)	0.2
Flip	Horizontal/Vertical
Fill mode	Nearest

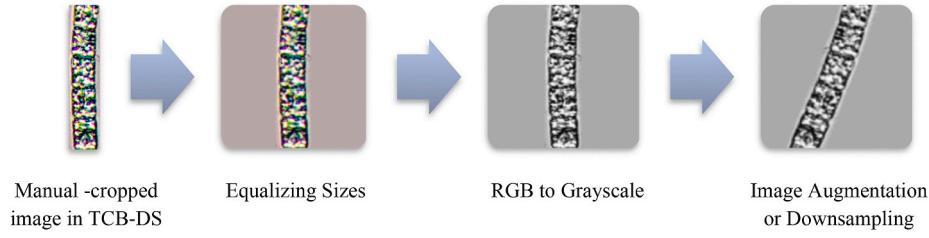


Fig. 2. Preprocessing of an *Aphanizomenon* sample from the training set of TCB-DS.

preprocessing steps is shown in Fig. 2.

$$P_{\text{Selection}}(X) = \frac{\text{mean}\left(\sum_{c \in C} N_c\right)}{N_{X_c}} + K \cdot \begin{cases} C : \text{different classes in dataset} \\ N_c : \text{count of samples of class } c \text{ in dataset} \\ N_{X_c} : \text{count of samples in class of sample } X \\ K : \text{constant real number between 0 and 1} \end{cases} \quad (1)$$

### 13. Model architectures

In this section, despite the fact that many methods with different parameters were evaluated, only one method that had acceptable accuracies is explained. This method had two parts. The first step is feature extraction which uses some models to extract a vector representation of each image. The vector representation of an image is a vector of specified length e.g., 100., consisting of the feature of the image. Vector representation of an image is preferred to the original image for classification purposes as is less in dimension and easier to classify. In the second step, some classification models were performed to assign the resulting extracted features to TCB\_DS unique classes. In the feature extraction phase, some pre-trained models were used to extract features from images. Instead of initializing the weights of the models randomly and learning them from scratch, we set pre-trained weights to them and

fine-tune them as shown in Fig. 3. In other words, the method that will be discussed has employed the concept of transfer learning to extract features. According to Table 2, there are just 2852 images in the training set even after augmentation; Thus, transfer learning approaches were preferred to building models from scratch as using pre-trained models requires less training data and less computational time (Zhao et al., 2024).

As is shown in Fig. 3, the source model is a model such as MobileNet, VGG16, etc. Trained before with a large source dataset such as ImageNet (Deng et al., 2009) and the target model is the same as the source model with the source model weights, with a difference that it is fine-tuned with the TCB-DS. In the fine-tuning phase, often the learning rate of initial layers is a small number or zero (freeze layers) and the latest layers have a larger learning rate.

In addition to classification with FCNN after the pre-trained layers of the CNN model, in the classification phase of the proposed method, some classification models such as SVM, KNN, MLP, FCNN, XGBoost, RF, NB, etc. Were used for classification with the input of extracted features from the fine-tuned CNN models. In most cases, using an FCNN led to better results. It is noteworthy that a classifier model learns from the extracted features which the fine-tuned CNN based models extracted from training data.

In the test phase, the models which are for feature extraction have fed with an input test image. These models extract some vectors with a certain dimension (for example 100) which can often carry the characteristic of the image. Afterward, the models which are for classification, get the extracted features of the test image and assign them to a genus of

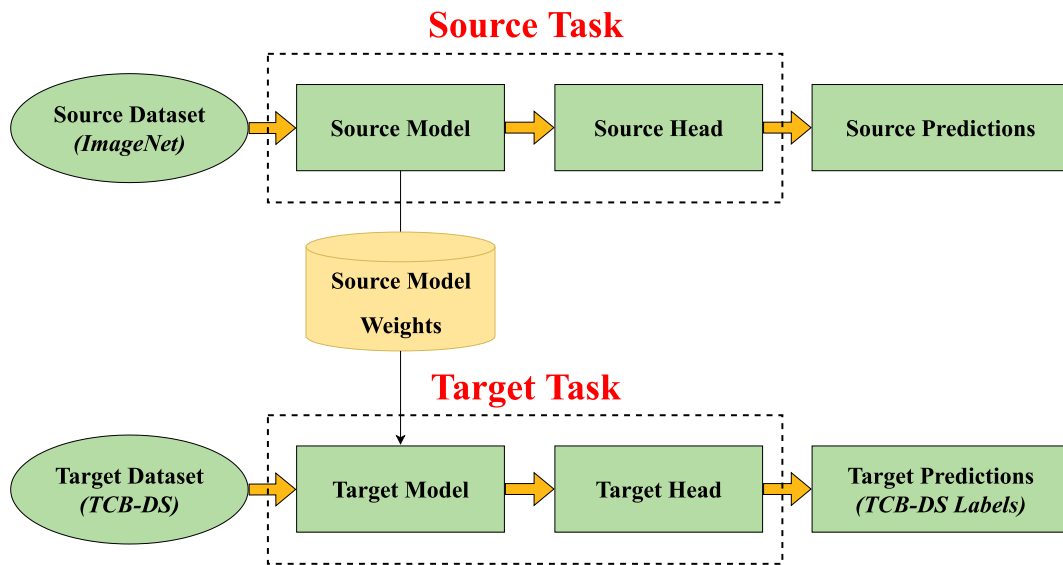


Fig. 3. Transfer Learning approach instead of training from scratch. The above row shows training a model from scratch with a large dataset e.g., ImageNet and the second row shows that the trained model in the first row was used for a new task after fine-tuned.

Cyanobacteria.

In this study, only MobileNet and MobileNetV2 were examined to extract the features because the MobileNet model brings the most weighted accuracy and the MobileNetV2 model brings the most macro accuracy and also some classification methods like SVM, KNN, MLP, FCNN, XGBoost, RF, NB were performed and examined deeply for classification part.

#### 14. Feature Extraction

**Feature Extraction – MobileNet.** The MobileNet model is TensorFlow's first mobile computer vision model, and as its name suggests, it is designed for use in mobile applications. MobileNet makes use of depthwise separable convolutions, and in fact, depthwise convolution and convolution are merged to form a depthwise separable convolution. When compared to a network with conventional convolutions of the same depth in the nets, it dramatically reduces the number of parameters. The architecture of MobileNet that was used in this model is shown in Table S3 (Howard et al., 2017).

As shown in Table S3, the MobileNet and the last layers totally have 3,262,363 parameters which 3,240,474 among them are trainable parameters. Instead of initializing the parameters randomly, the weights of trained MobileNet on the ImageNet dataset are used and after that fine-tuned with the TCB-DS, the Adam optimization algorithm and a scheduling learning rate starting at 0.001. Learning rate schedules adjust the learning rate during the training of the model by reducing the learning rate in accordance with a pre-defined schedule function. As can be seen in Figure S2, the learning rate at the early epochs was 0.001 and after some epochs, the learning rate was decreasing exponentially. Scheduling learning rate helps the optimization algorithm to converge to a better optimum because, over epochs, it reduces the learning rate and prevents divergence. The learning rate formula used in this paper is shown in Eq. (2).

$$LR = \begin{cases} LR & \text{if epoch} \leq 5, \\ LR \times e^{-0.1} & \text{otherwise} \end{cases} \quad (2)$$

The certain hyper-parameters of the model for fine-tuning are shown in Table S4. It is obvious that during fine-tuning the last layer of the model should have softmax activation function and 10 outputs that are including the probabilities that an input image belongs to each of the 10 classes of Cyanobacteria in TCB-DS. So an argmax on the probabilities of the last layer gives the assigned category for the input image. It is mentionable that the latest FCNN layers are for classification purposes and not necessary for feature extraction but in the fine-tuning phase, their existence is critical because they allow the feature extraction model to be fine-tuned by calculating the cross-entropy loss function on the last layer of FCNN which have a dimension of 10.

As is shown in Table S4, the categorical cross-entropy loss function which is defined in Eq. (3), was used in this method.

$$\text{Loss} = - \sum_{i=1}^{\text{output size}} y_i \bullet \log \hat{y}_i \quad (3)$$

**Feature Extraction – MobileNetV2.** A convolutional neural network design called MobileNetV2 introduced in 2018 by Google aims to perform well on mobile devices. It is built on an inverted residual structure where the bottleneck layers are connected by residual connections. Lightweight depthwise convolutions are used in the intermediate expansion layer as a source of non-linearity to filter features. The architecture of MobileNetV2 includes a 32-filter initial fully convolution layer as well as 19 additional bottleneck layers. MobileNetV2 was achieved 90.1% Top-5 accuracy for ImageNet while MobileNet had been achieved 89.5% Top-5 accuracy for ImageNet. Paper (Sandler et al., 2018), has studied the architecture of MobileNetV2 and its comparison

with other CNN based deep neural networks such as MobileNet by depth.

In the second feature extraction model of this paper, the pre-trained MobileNetV2 - which was trained previously on ImageNet - was used which had 1,997,402 trainable parameters for fine-tuning among a total of 2,299,674 parameters because all layers except the last 60 layers of the MobileNetV2 were frozen (set learning rate of layers to zero). First, the pre-trained MobileNetV2 was fine-tuned with the training set of TCB-DS. The hyperparameters for fine-tuning MobileNetV2 are like the first model (MobileNet) fine-tuning hyperparameters, only the learning rate starts from 0.0001 instead of 0.001 to prevent divergence in the first epochs (Table S5).

#### 15. Classification

**Classification – FCNNs.** After the previous section which was about feature extraction with the fine-tuned models such as MobileNet and MobileNetV2, a classification model is needed to recognize different types of Cyanobacteria from extracted features. Two different approaches were applied after feature extraction. In the first approach, some FCNN come after the feature extraction was used to classify the images. In fact after the main layers of the feature extraction models, a global max pooling layer was performed to extract a feature vector from the 2D feature maps of an input image. After applying global max pooling, three dense layers with 32,16 and 10 nodes were applied to do classification which was named baseline CNN. The activation function of the first and second layer is adam and the last layer is softmax. The training of these layers did during fine-tuning of feature extraction models. In fact, the FCNN parameters were trainable in fine-tuning step. A summary diagram of this approach is shown in Fig. 4.

**Classification – Classic algorithms.** In the second approach for classification, after fine-tuning the feature extraction models, layers of these models were used for feature extraction from input images. The flatten layers were used at the end of convolution layers of the feature extraction model to convert some 2D feature maps of a image to a flattenfeature vector. After that, a Principal Component Analysis (PCA) with 100 principal components was applied to flatted features vector -which were extracted from input images - for dimensionality reduction. After applying PCA, only one vector with a dimension of 100 was obtained for each image in the training and test set. After these 100-dimensional vectors were obtained for all images of the training and test set, several classic classification algorithms such as SVM were used to classify them to one genus. The hyperparameters of these classifiers are mentioned in Table 4 and a summary diagram of this approach is shown in Fig. 5.

As will be mentioned in the result section, the combination of using MobileNet for feature extraction and FCNN for classification had the best weighted accuracy and the combination of using MobileNetV2 and FCNN had the best macro accuracy. Then, the best approach for classification among two mentioned approaches is the first one, which used FCNN after the end of the layers of the feature extraction model.

#### 16. Results

##### 16.1. Evaluation metrics

Two performance evaluation criteria including weighted and macro criteria studied in this paper. Each criterion has three sub-criteria such as precision, recall, and F1-score and has some information and some analysis which in this section are studied. The criterion of recognition accuracy used to evaluate the offered approaches is defined as Eq. (4):

$$\text{Accuracy} = \frac{TP + TN}{TP + TN + FP + FN} \quad (4)$$

Several regularly used metrics, aside from accuracy, like precision, recall, and F1-score are defined as Eqs. (5)–(7) to provide more

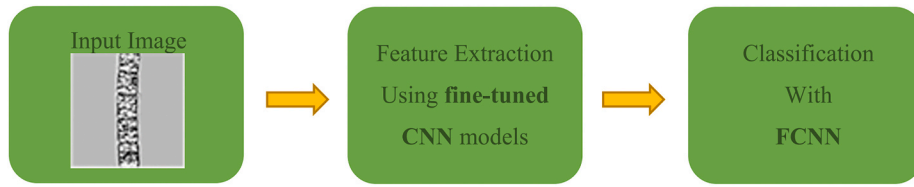


Fig. 4. Summary of the first approach for classification.

Table 4

Classic classification algorithms and their hyper-parameters.

Classification algorithm	Hyper parameters
SVM	RBF kernel
Naïve Bayes	Gaussian NB
MLP	1 Layer, 100 Hidden nodes
XGBoost	–
Random Forest	Max depth = 100
KNN	K = 3

information about the performance of each method and to increase method comparability:

$$\text{Precision} = \frac{TP}{TP + FP} \quad (5)$$

$$\text{Recall} = \frac{TP}{TP + FN} \quad (6)$$

$$F1 - \text{Score} = \frac{2 \times \text{Precision} \times \text{Recall}}{\text{Precision} + \text{Recall}} \quad (7)$$

It is mentionable that the above criteria are calculated separately for each class with the OneVsAll concept. Then, macro criteria are defined as Eqs. (8)–(10) and the weighted criteria is defined as Eqs. (11)–(13):

$$\text{Precision}_{\text{Macro}} = \sum_{c \in \text{classes}} \frac{\text{Precision of class } c}{\text{Number of classes}} \quad (8)$$

$$\text{Recall}_{\text{Macro}} = \sum_{c \in \text{classes}} \frac{\text{Recall of class } c}{\text{Number of classes}} \quad (9)$$

$$F1 - \text{Score}_{\text{Macro}} = \sum_{c \in \text{classes}} \frac{\text{Recall of class } c}{\text{Number of classes}} \quad (10)$$

$$\text{Precision}_{\text{Weighted}} = \sum_{c \in \text{classes}} \text{weight of class } c \times \text{Precision of class } c \quad (11)$$

$$\text{Recall}_{\text{Weighted}} = \sum_{c \in \text{classes}} \text{weight of class } c \times \text{Recall of class } c \quad (12)$$

$$F1 - \text{Score}_{\text{Weighted}} = \sum_{c \in \text{classes}} \text{weight of class } c \times F1 - \text{Score of class } c \quad (13)$$

## 16.2. Experimental settings

The feature extraction and classification processes were implemented in the Jupyter notebook. The experiments were done on a Google Colab account. It provided a Tesla T4 GPU, equipped with 15 GB of GPU RAM. Despite this, the accessible main RAM was restricted to just 13 GB.

## 16.3. Comparative analysis

Table 5 provides a summary of the mentioned research works. This table shows that CNNs are more frequently used in studies conducted in recent years. Indeed, it demonstrates that CNN models extract the features of images better than traditional methods such as PCA and because of this point, classification models that used CNNs in the feature extraction phase mostly achieved more accurate results. Additionally, this table depicts that transfer learning approaches perform well for modeling datasets containing many images. However, the methods and the results cannot be directly compared based on the results of the table because of the wide variation in datasets and tasks. For example, Sonmez et al. (2022) worked on a dataset with only two labels. So, the results of this paper cannot be compared with our result with 10 labels. In other more similar studies, we cannot compare the results too because of variations and situations of gathering datasets. To compare the results, the source codes should be applied to the same selected public datasets but since their codes mostly are not publicly available, the comparison is also unfeasible.

## 16.4. Complementary results

Several models for feature extraction and classification were assessed and two combinations with the highest weighted accuracy and macro accuracy are explained deeply. In this section, the results of selecting each model for feature extraction and detailed analysis are reported.

## 16.5. Results of applying MobileNet

Table S6 displays the results of applying the first proposed feature extraction model (fine-tuned MobileNet) on the test set of TCB-DS considering all the classes and the images. The combination of this model and the CNN for classification, has the highest weighted accuracy, precision, recall, and F1-score by 94.79%, 95.34%, 94.79%, and 94.91%. The results of a model which was created with the combination

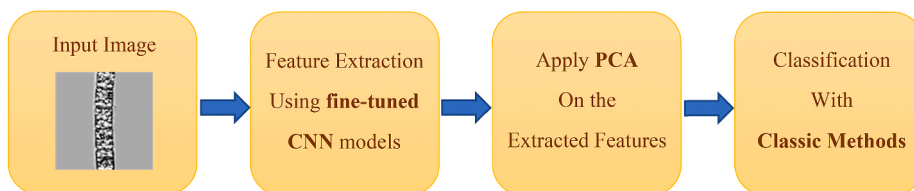


Fig. 5. Summary of using classic methods for classification.



**Table 5**

Previous works on bacterial image classification. All of the methods except the first three methods that use shape features, extract deep features to classify bacteria.

Methodology	Type of Bacteria	Dataset	Accuracy	Author/Year
KNN	Bacterial Morphotypes	Digital Images	97%	Liu et al. (Liu et al., 2001)
SMO	Microalgae genera	Digital Images	97.22%	Promdaen et al. (Promdaen et al., 2014)
PCA + BPNN	Wastewater Bacteria	NMCR database	86.30%	Xiaojuan et al. (Xiaojuan and Cunshe, 2009)
CNN	Mycobacterium Tuberculosis	Digital Images	99%	Lopez et al. (Yadini Pérez López et al., 2017)
CNN (InceptionV1)	Pathogenic Bacteria	HOWMED, PIXNIO	95%	Wahid et al. (Md Ferdous Wahid et al., 2018)
SVM, RF CNNs, FV	General Bacteria Species	DIBaS	97.24%	Zielinski et al. (Zieliński et al., 2017)
CNN (AlexNet)	General Bacteria Species	DIBaS	98.22%	Khalifa et al. (Khalifa et al., 2019)
CNN (VGG-16, AlexNet)	General Bacteria Species	DIBaS	98.25%	Nasip et al. (Nasip and Zengin, 2018)
CNN (ResNet50)	General Bacteria Species	DIBaS	99.20%	M. Talo (Talo, 2019)
CNN (ResNet50)	General Bacteria Species	DIBaS (20 out of 33 classes)	99.90%	Shaily et al. (Shaily and Kala, 2020)
NAS + CNN	Algal genera in watersheds experiencing algal blooms	Digital Microscopic Images (private)	95.63% (F1-Score)	Park et al. (Park et al., 2019)
MLP	Algae types	Digital Microscopic Images (private)	96.1%	Deglint et al. (Deglint et al., 2019)
R-CNN + CNN	Cyanobacteria	Digital Microscopic Images (private)	90.22%	Baek et al., 2020
CNN + SVM	Cyanobacteria and Chlorophyta groups	Digital Microscopic Images (private)	99.66%	Sonmez et al. (Sonmez et al., 2022)
CNN + FCNN (Alex-VGG)	Cyanobacteria	Digital Microscopic Images (private)	99.36%	Gaur et al. (Gaur et al., 2022)
Faster R-CNN + RetinaNet + FPN + CNN	Phytoplankton Specimens	FMPD	76.39%	Figueroa et al. (Figueroa et al., 2024)
CNN + Transformer	Infectious bacteria	Digital Microscopic Images (private)	99.44%	Lu et al. (Lu et al., 2024)
CNN	Desmids	Digital Microscopic Images (private)	99%	Pardeshi et al. (Pardeshi and Deshmukh, 2023a)
CNN	General algae	Digital Microscopic Images (private)	99%	Pardeshi et al. (Pardeshi and Deshmukh, 2023b)
CNN	General algae	Digital Microscopic Images (private)	97.27%	Otalora et al. (Otalora et al., 2023)
CNN (MobileNet)	Toxigenic Cyanobacteria genera	TCB-DS (publicly available)	94.91%	Ours (CBCB)

of the MobileNet for feature extraction and the FCNN for classification was shown in Table S7. The accuracies were calculated through the OneVsAll manner for each class separately. The Precision, Recall, F1-Score, and Weight are the metrics used for evaluating the accuracy of detection. The Precision measures the percentage of correct positive predictions among all positive predictions, while Recall measures the percentage of correct positive predictions among all true positives. F1-Score is the harmonic mean of Precision and Recall, and Weight indicates the number of samples for each genus.

The results in Table S7 imply that if the classes which have less than 10 test samples (*Aphanizomenon*, *Cylindrospermopsis* and *Raphidiopsis*) are deleted from the calculation, the accuracy will be increased significantly especially for Macro criteria.

The confusion matrix of this model (MobileNet + FCNN) is shown in Figure S3 and Figure S4, depicts the process of loss and accuracy changes throughout 40 training epochs.

#### 16.6. Results of applying MobileNetV2

The results of applying the second feature extraction model (tuned MobileNetV2) on the test set of TCB-DS while taking into account all classes and images are shown in Table S8.

By comparing Table S6 and Table S8 it is clear that the second combination (MobileNetV2 + FCNN) is more accurate if macro criteria was selected. The macro precision, recall and f1-score in this method is 87.74, 90.17 and 87.64. By Table S9, it is easy to understand the reason why these accuracies are higher compared to the model that used MobileNet in its feature extraction phase (first combination).

The result of the comparison of Table S7 and Table S9 is that the accuracy in the second model has increased in the classes with low accuracy, but the high accuracy has decreased for the classes that have more samples. It implies that the performance values related to

weighted criteria are higher in the first model while the performance values related to the macro criteria are better in the second. The confusion matrix of the second model which used MobileNetV2 for feature extraction and FCNN for classification is shown in Figure S5.

The process of changes in the accuracy and loss of the training, validation, and test sets per epoch during the training phase of the second model are shown in Figure S6.

Although the main evaluation criterion is the weighted criterion and the first model which used fine-tuned MobileNet is the best in this type of accuracy, macro accuracy may be required in some applications. In this case, it is better to use the second model (MobileNetV2), which has higher macro accuracy.

Some other pre-trained models were tested, such as VGG16, Xception, etc., and the accuracy results of these tested models are presented in Table 6. In this paper, two of these models that had the highest accuracy in terms of macro and weighted criteria were studied, and the rest of the tests can be seen in Table 6.

#### 16.7. Some classified and misclassified images

Table S10 shows some correct and wrong predictions of the first model which is an image fed to fine-tuned MobileNet and its resulting extracted features are fed to the FCNN to assign it to one of 10 genera. The images in Table S10 are from test set of TCB-DS.

### 17. Discussion

Microbial morphology can be analyzed using image processing to distinguish between different bacterial genera, classify them, and even identify them. Recent advances in AI-based computer vision have made it possible to automate bacterial image recognition, enabling more rapid and precise detection.

**Table 6**

Performance of different pre-trained models in this study.

Feature Extraction	Dimentionality reduction	Classifier	Accuracy (%)	Precision (%)	Recall (%)	F1-Score (%)	Macro Precision (%)	Macro Recall (%)	Macro F1-Score (%)	Hyper Parameters
<b>MobileNet (Model 1)</b>	PCA with 100 components	SVM	0.926,640,927	0.9429	0.9266	0.9276	0.8303	0.8378	0.8133	Kernel = rbf; Learning rate schedule = 0.001; 40 epochs
		XGBoost	0.8,996,139	0.9191	0.8996	0.8977	0.696	0.7615	0.7095	Learning rate schedule = 0.001; 40 epochs
		Random Forest	0.920,849,421	0.9349	0.9208	0.9215	0.8299	0.8313	0.8124	Max_depth = 100; Learning rate schedule = 0.001; 40 epochs
		Naïve Bayes	0.909,266,409	0.927	0.9093	0.9096	0.7142	0.743	0.7178	Gaussian; Learning rate schedule = 0.001; 40 epochs
		KNN	0.920,849,421	0.9333	0.9208	0.9211	0.8287	0.829	0.8099	n_neighbors = 3; Learning rate schedule = 0.001; 40 epochs
		MLP	0.922,779,923	0.9334	0.9228	0.9223	0.8312	0.8283	0.8111	max_iter = 300; Learning rate schedule = 0.001; 40 epochs
	–	<b>FCNN</b>	<b>0.947876453</b>	<b>0.9534</b>	<b>0.9479</b>	<b>0.9491</b>	<b>0.8502</b>	<b>0.8483</b>	<b>0.8353</b>	Learning rate schedule = 0.001; 40 epochs
	PCA with 100 components	SVM	0.915,057,915	0.9228	0.9151	0.916	0.8623	0.8942	0.8658	Kernel = rbf; Learning rate schedule = 0.001; 40 epochs
		XGBoost	0.907,335,907	0.9182	0.9073	0.9086	0.7732	0.8823	0.8052	Learning rate schedule = 0.001; 40 epochs
		Random Forest	0.915,057,915	0.9227	0.9151	0.916	0.8634	0.8911	0.865	Max_depth = 100; Learning rate schedule = 0.001; 40 epochs
		Naïve Bayes	0.878,378,378	0.912	0.8784	0.8849	0.8333	0.8211	0.7971	Gaussian; Learning rate schedule = 0.001; 40 epochs
		KNN	0.922,779,923	0.9283	0.9228	0.9237	0.8656	0.8968	0.8659	n_neighbors = 3; Learning rate schedule = 0.001; 40 epochs
		MLP	0.911,196,911	0.9189	0.9112	0.9124	0.7865	0.8879	0.8245	max_iter = 300; Learning rate schedule = 0.001; 40 epochs
	–	<b>FCNN</b>	<b>0.928571403</b>	<b>0.9331</b>	<b>0.9286</b>	<b>0.9293</b>	<b>0.8774</b>	<b>0.9017</b>	<b>0.8764</b>	Learning rate schedule = 0.001; 40 epochs
VGG16 (3 last layers were not freeze)	PCA with 100 components	SVM	0.8,996,139	0.9122	0.8996	0.9006	0.679	0.7564	0.7038	Kernel = rbf; Learning rate schedule = 0.001; 40 epochs
		XGBoost	0.874,517,375	0.9004	0.8745	0.8772	0.6566	0.7366	0.6762	Learning rate schedule = 0.001; 40 epochs
		Random Forest	0.891,891,892	0.9076	0.8919	0.8942	0.6597	0.7479	0.6872	Max_depth = 100; Learning rate schedule = 0.001; 40 epochs
		Naïve Bayes	0.847,490,347	0.8826	0.8475	0.8561	0.6277	0.7017	0.6401	Gaussian; Learning rate schedule = 0.001; 40 epochs
		KNN	0.891,891,892	0.9036	0.8919	0.8932	0.6804	0.7437	0.6985	n_neighbors = 3; Learning rate schedule = 0.001; 40 epochs
		MLP	0.874,517,375	0.897	0.8745	0.8771	0.6423	0.7322	0.6627	max_iter = 300; Learning rate schedule = 0.001; 40 epochs

(continued on next page)

Table 6 (continued)

Feature Extraction	Dimentionality reduction	Classifier	Accuracy (%)	Precision (%)	Recall (%)	F1-Score (%)	Macro Precision (%)	Macro Recall (%)	Macro F1-Score (%)	Hyper Parameters
DenseNet121 (70 last layers were not freeze)	–	<u>FCNN</u>	<u>0.911196887</u>	<u>0.9166</u>	<u>0.9112</u>	<u>0.9114</u>	<u>0.6935</u>	<u>0.7659</u>	<u>0.7207</u>	Learning rate schedule = 0.001; 40 epochs
	PCA with 100 components	SVM	0.924,710,425	0.9312	0.9247	0.925	0.6956	0.7507	0.7156	Kernel = rbf; Learning rate schedule = 0.001; 40 epochs
		XGBoost	0.88,996,139	0.9015	0.89	0.8907	0.6801	0.7184	0.6908	Learning rate schedule = 0.001; 40 epochs
		Random Forest	0.905,405,405	0.9166	0.9054	0.9292	0.6604	0.7257	0.6815	Max_depth = 100; Learning rate schedule = 0.001; 40 epochs
		Naïve Bayes	0.897,683,398	0.9132	0.8977	0.9013	0.6574	0.7342	0.6819	Gaussian; Learning rate schedule = 0.001; 40 epochs
		KNN	0.928,571,429	0.9362	0.9286	0.9299	0.7033	0.7734	0.7255	n_neighbors = 3; Learning rate schedule = 0.001; 40 epochs
		MLP	0.920,849,421	0.9297	0.9208	0.9231	0.6826	0.7458	0.7028	max_iter = 300; Learning rate schedule = 0.001; 40 epochs
InceptionV3 (40 last layers were not freeze)	–	<u>FCNN</u>	<u>0.930501938</u>	<u>0.9377</u>	<u>0.9305</u>	<u>0.9308</u>	<u>0.7115</u>	<u>0.7853</u>	<u>0.7371</u>	Learning rate schedule = 0.001; 40 epochs
	PCA with 100 components	<u>SVM</u>	<u>0.905405405</u>	0.9114	<u>0.9054</u>	0.9054	<u>0.7808</u>	<u>0.7513</u>	<u>0.7517</u>	Kernel = rbf; Learning rate schedule = 0.001; 40 epochs
		XGBoost	0.83,011,583	0.8648	0.8301	0.9353	0.5914	0.6196	0.587	Learning rate schedule = 0.001; 40 epochs
		Random Forest	0.893,822,394	0.9104	0.8938	0.8977	0.6475	0.7195	0.6664	Max_depth = 100; Learning rate schedule = 0.001; 40 epochs
		Naïve Bayes	0.88,996,139	0.8995	0.89	0.8908	0.6735	0.6816	0.6681	Gaussian; Learning rate schedule = 0.001; 40 epochs
		KNN	0.905,405,405	0.9104	<u>0.9054</u>	0.9047	0.753	0.7256	0.727	n_neighbors = 3; Learning rate schedule = 0.001; 40 epochs
		MLP	0.903,476,903	0.9055	0.9035	0.9025	0.6663	0.7001	0.6798	max_iter = 300; Learning rate schedule = 0.001; 40 epochs
Xception (7 last layers were not freeze)	–	<u>FCNN</u>	0.903,474,927	<u>0.9123</u>	0.9035	0.9049	0.7736	0.7439	0.7421	Learning rate schedule = 0.001; 40 epochs
	PCA with 100 components	SVM	0.901,544,402	0.9049	0.9015	0.9015	0.7046	0.747	0.7202	Kernel = rbf; Learning rate schedule = 0.001; 40 epochs
		XGBoost	0.878,378,378	0.8927	0.8784	0.8814	0.6337	0.7135	0.6588	Learning rate schedule = 0.001; 40 epochs
		Random Forest	0.893,822,394	0.8991	0.8938	0.8946	0.6641	0.7178	0.6848	Max_depth = 100; Learning rate schedule = 0.001; 40 epochs
		Naïve Bayes	0.855,212,355	0.8722	0.8552	0.8583	0.6351	0.7221	0.6642	Gaussian; Learning rate schedule = 0.001; 40 epochs
		KNN	0.897,683,398	0.9014	0.8977	0.8979	0.7202	0.7203	0.7125	n_neighbors = 3; Learning rate schedule = 0.001; 40 epochs
		MLP	<u>0.907335907</u>	<u>0.9131</u>	<u>0.9073</u>	<u>0.9079</u>	<u>0.7318</u>	<u>0.7308</u>	<u>0.7221</u>	max_iter = 300; Learning rate

(continued on next page)

Table 6 (continued)

Feature Extraction	Dimentionality reduction	Classifier	Accuracy (%)	Precision (%)	Recall (%)	F1-Score (%)	Macro Precision (%)	Macro Recall (%)	Macro F1-Score (%)	Hyper Parameters
	–	FCNN	0.895,752,907	0.8995	0.8958	0.8963	0.6875	0.7137	0.6962	schedule = 0.001; 40 epochs Learning rate schedule = 0.001; 40 epochs

Cyanotoxins are toxic metabolites produced by Cyanobacteria in water resources and can cause a range of symptoms including skin irritation, respiratory problems, liver damage, and even death in severe cases. Long-term exposure to low levels of cyanotoxins has also been linked to an increased risk of cancer (Svirčev et al., 2017).

The level of cyanotoxins in water resources must be taken into consideration in the panel of quality control measures due to the health risks associated with high levels of cyanotoxins in drinking or agricultural water resources. According to World Health Organization (WHO), there is a fair level of risk that is in waters in which concentrations of cyanobacterial cells reaching or surpassing 100,000 cells per mL will have harmful health effects on individuals (Organization, 2003). However, the population in a given water sample may not necessarily contain toxigenic cyanobacterial genera, and therefore the cell number threshold defined by agencies may not be an accurate indicator of water toxicity. Moreover, Cyanobacteria typically have filamentous cells, therefore counting them manually is an inaccurate estimation. In addition, another challenge in the enumeration of Cyanobacteria is that the analytical results do not provide information about the specific type of cyanobacterial genera. As a result, it becomes difficult to distinguish between harmful and non-toxicogenic genera (Chiu et al., 2017).

The computational models for analyzing imaging and non-imaging flow cytometry images of microorganisms aim to mostly identify and also quantify types of microorganisms in water samples based on their optical properties (Safford and Bischel, 2019). However, as high-tech devices are not available in most water quality control units specially in rural areas, the introduction of an approach for screening the water sample based on their microscopic slides is valuable. Thus, the integration of AI-based image recognition techniques can significantly enhance the rapid and precise detection of toxigenic cyanobacterial genera.

Our CNN-based model for classification of Cyanobacteria, though similar to (Gaur et al., 2022) in using deep learning, differs significantly in its approach. Unlike their fusion of AlexNet and VGG16 features, we employed either MobileNet or MobileNetV2 for feature extraction and tackled class imbalance with resampling techniques rather than cross-validation. Both studies underscore the efficacy of deep learning in cyanobacterial classification, the performance of our model is comparable to the performance reported by Gaur et al. While Zeng et al. explored model generalization in satellite image analysis (Zeng et al., 2022), our study faces challenges related to the small size and variability of our training set, TCB-DS. Despite these issues, we leveraged transfer learning with pre-trained CNNs to enhance model generalizability, aiming to overcome limitations similar to those Zeng et al. identified in large-scale datasets. This approach allowed us to adapt knowledge from extensive datasets to the niche task of cyanobacteria classification.

The acceptable identification of toxigenic cyanobacterial genera enabled by our model can inform decision-making processes in water resource management, allowing for more targeted and effective treatment strategies. (Svirčev et al., 2017). In the context of Cyanobacteria detection and classification, the choice of evaluation metrics is crucial as it directly impacts the biological interpretability and practical applicability of the model's output. The choice of evaluation metrics can be tailored to specific water quality management objectives. For instance, in scenarios where the primary concern is identifying the presence of any toxigenic genera, prioritizing recall over precision could be more

appropriate. Conversely, in situations where resource allocation and treatment costs need to be optimized, higher precision may be preferred to minimize false positives and unnecessary interventions. The results of our proposed model indicate that the genus with the highest precision and recall scores was *Microcystis* with a perfect precision score of 1.0000 and a recall score of 0.9787, resulting in an F1-score of 0.9892, which is among the most common toxigenic genus in freshwater ecosystems. The second most accurately detected genus is *Nostoc* with a precision score of 0.9733 and a perfect recall score of 1.0000, resulting in an F1-score of 0.9865. Higher accuracy of *Microcystis* can be attributed to the richer used dataset while the accuracy of the detection of *Nostoc* members can more be associated with their higher intricate cellular features. The excellent precision and recall scores achieved for *Microcystis* and *Nostoc* genera are particularly significant, as these genera are known to produce potent hepatotoxins (microcystins) and neurotoxins (anatoxin-a), respectively.

Higher accuracy of *Microcystis* can be attributed to the richer used dataset while the accuracy of the detection of *Nostoc* members can more be associated with their higher intricate cellular features. The excellent precision and recall scores achieved for *Microcystis* and *Nostoc* genera are particularly significant, as these genera are known to produce potent hepatotoxins (microcystins) and neurotoxins (anatoxin-a), respectively. There was no essentially direct correlation between the number of training dataset and obtained accuracy, as some genera with low weight have high accuracy, such as *Raphidiopsis*, which has a weight of 2 but a precision of 1.0. The results suggests that the accuracy of detection depends on the specific micromorphological feature of the taxon genus being analyzed and cannot be generalized across all genera.

As discussed earlier, many of state of art studies have used CNN-based models and transfer learning approaches due to small training sets. In this study, we also used transfer-learning based approaches because of the small size of TCB-DS. A MobileNet pre-trained model was used and a weighted f1-score of 94.91% was achieved as the best-weighted f1-score and a pre-trained MobileNetV2 was used and the macro f1-score of 87.64% was attained as the best macro f1-score. The classification of this study indicates that *Microcystis* and *Nostoc* were the most accurately detected genera, while *Aphanizomenon* had the lowest F1-score. Higher accuracy of *Microcystis* can be attributed to the richer used dataset while the accuracy of the detection of *Nostoc* members can more be associated with their higher intricate cellular features. It suggests that a more targeted approach or a higher diversity or number of training micrographs may be needed to accurately detect specific types of Cyanobacteria. The liver cyanotoxin of cylindrospermopsin produced by *Aphanizomenon* strains are often intracellular opposite to the most others which are secretory and thus the concern on their detection with slightly less accuracy is less compared to other toxigenic strains. However, follow up studies must work to increase the accuracy of the *Aphanizomenon* strains as they produce extracellular neurotoxins of saxitoxins and Beta-Methylamino-L-alanine (BMAA) that is probably implicated in initiation of neurodegenerative disorders and even low abundances of *Aphanizomenon* can lead to cylindrospermopsin, saxitoxin and BMAA accumulation in water bodies (Lyon-Colbert et al., 2018).

The most successful model for feature extraction from cyanobacterial images was found to be MobileNet. Different methods for classification of the features extracted from CNN models were tested, and the results showed that a fully connected neural network (FCNN) after the



convolution layers of fine-tuned MobileNet can predict the toxigenic genera with weighted accuracy and f1-score of 94.79% and 94.91%, respectively. The highest macro accuracy and f1-score of 90.17% and 87.64% were obtained using MobileNetV2 for feature extraction. Overall, the presented models were able to classify the toxigenic cyanobacterial genera with an F1-score of 95%, suggesting the possible applicability of CNN for the recognition of toxigenic Cyanobacteria in practice.

The observed variations in detection accuracy among genera suggest that the model's performance is influenced by the specific morphological characteristics of cyanobacterial cells. For instance, the filamentous nature of *Nostoc* and the characteristic cellular arrangements of *Microcystis* colonies may have contributed to their higher detection rates. Conversely, genera with more subtle or variable morphologies, like *Aphanizomenon*, could benefit from additional training data to capture their diverse cellular features.

While our model relies solely on morphological features extracted from microscopic images, integrating this approach with molecular data, such as toxin gene expression or metabolomic profiles, could further enhance the accuracy and informativity of cyanobacterial identification. By combining visual cues with molecular signatures, it may be possible to differentiate between toxic and non-toxic strains within the same genus, providing a more comprehensive assessment of potential health risks.

The limitations in our study include: First, limited scope: our study focused on the detection of 10 specific cyanobacterial genera that are capable of producing more than two types of cyanotoxins. Moreover, it is possible that some Cyanobacteria species within these genera found in a specific water sample may not produce any toxin due to genetic changes or lack of expression of biosynthetic genes (Neilan et al., 2013). Furthermore, some cyanobacterial genera are in low abundance and thus may not be observed in microscopic fields of water samples (Paerl and Huisman, 2008). It is also possible that a single species of Cyanobacteria in a water sample may generate a high concentration of toxins, which could be lethal if not accurately detected or enumerated through image analysis.

When toxin biosynthetic clusters are silent, the model may produce false-positive predictions, or conversely, a single strain of Cyanobacteria in a water sample may produce a concentration of toxins above the threshold, resulting in false negatives.

Our analysis faced challenges due to the heterogeneous nature of the image scales and resolutions within our multi-site dataset, leading to decreased accuracy. This variability, rather than a deficiency in our methodology, underscores the complexity of our dataset and the rigorous conditions under which our model was evaluated.

Second, small training set and data limitations: Our study utilized a small set of microscopic images from only 10 genera (1200 before manual cropping and 2073 afterward). The number of trainsets in some genera very not enough to represent the modeling of that genus. In addition, this number of learning data were not enough for training a deep neural network algorithm from scratch. While the model was trained and validated using data from the TCB-DS dataset, its performance could vary when applied to samples from other regions or under different environmental conditions. Additionally, due to the small size of the training set, pre-trained CNN models were utilized to aid in classification and analysis, which may limit the ability to fine-tune the model for specific features of the training set.

Several avenues can be explored to further enhance the accuracy and robustness of the proposed Cyanobacteria classification method. Future studies could investigate different preprocessing techniques to reduce image noise and simplify the models, thereby strengthening their performance. One promising approach is the utilization of patch-based cropping techniques for image preprocessing. By dividing the input images into smaller, distinct patches, the model's trainable parameters can be reduced, as the size of the model is directly related to the input image dimensions.

Another potential avenue for improvement lies in the incorporation of attention mechanisms into the neural network architecture. Attention mechanisms have demonstrated remarkable success in various visual tasks, including image classification, by assigning different importance values to different regions of the image and emphasizing certain salient parts. In the context of the TCB-DS, where the shape and arrangement of cyanobacterial cells are crucial for accurate identification, attention-based models can be leveraged to emphasize the regions of interest (ROI) for each genus, potentially leading to improved classification performance.

Moreover, the utilization of appropriate pre-trained models can be beneficial for achieving more precise classification results. By training the base model on immense, related datasets (e.g., datasets of microscopic images) and subsequently fine-tuning it with the TCB-DS, the model's feature extraction capabilities can be enhanced, leading to more accurate and robust predictions.

Finally, exploration of novel models and pre-trained weights, such as vision transformers (ViT) (Dosovitskiy et al., 2020) that leverage attention mechanisms, could potentially surpass the performance of traditional CNN methods in certain cases.

As mentioned, despite the success of the models, some challenges were faced during the computational modeling phase due to the small size of the training set and the size of the images. To increase the accuracy of classifying different cyanobacterial genera, patch-based cropping of images can be used for the modeling section in future studies. This involves dividing images into several distinct patches, which leads models to have fewer trainable parameters and increases the probability of accurate predictions. Furthermore, attention-based models can be employed to emphasize the region of interest (ROI) in each class to produce better results. It is expected that using an appropriate pre-trained model that is trained with immense related datasets first and then fine-tuned with the TCB-DS will also improve the classification accuracy.

## 18. Conclusion

Water quality surveillance is crucial for public and environmental health, particularly due to the threats posed by cyanotoxins produced by Cyanobacteria in freshwater sources.

By the time of writing this paper, there is not any report on employing ML and DL approaches with public datasets for the classification of toxin-producing cyanobacterial genera in water samples. In the present study, we developed an automated recognition system to differentiate toxigenic cyanobacterial genera based on microscopic images using fine-tuned CNN models. To address this issue, In the present study, we developed an automated recognition system to differentiate toxigenic cyanobacterial genera based on microscopic images using fine-tuned CNN models. The study focused on 10 toxigenic cyanobacterial genera (*Anabaena*, *Aphanizomenon*, *Cylindrospermopsis*, *Dolichospermum*, *Microcystis*, *Nostoc*, *Oscillatoria*, *Phormidium*, *Planktothrix*, and *Raphidiopsis*) capable of producing more than two chemical types of toxins, which are potentially more harmful than other genera. The most successful model for feature extraction from cyanobacterial images was found to be MobileNet. Different methods for classification of the features extracted from CNN models were tested, and the results showed that a fully connected neural network (FCNN) after the convolution layers of fine-tuned MobileNet can predict the toxigenic genera with weighted accuracy and f1-score of 94.79% and 94.91%, respectively. The highest macro accuracy and f1-score of 90.17% and 87.64% were obtained using MobileNetV2 for feature extraction. Overall, the presented models were able to classify the toxigenic cyanobacterial genera with an F1-score of 95%, suggesting the possible applicability of CNN for the recognition of toxigenic Cyanobacteria in practice. The replacement of the MobileNet with its version 2 in the combined model with FCNN decreased the number of genera identified with low f1-score (lower than 0.7) from three to one genus. Table S9 presents the detailed detection

accuracy results for each cyanobacterial genus, obtained using the MobileNetV2 model for feature extraction and the FCNN for classification. However, the precise and quick automated classification of Cyanobacteria using microscopic images of water samples has been challenging for ML methods due to variations in cell diameters and heterogeneous micromorphology of Cyanobacteria. Our developed tool can assist trained specialists in analyzing the quality of water in water bodies, which can significantly improve the efficiency and precision of the process for detection of harmful Cyanobacteria. By the approach presented in this research, the process of managing the water systems would no longer need to be done by individual specialists in future who are prone to make mistake, and besides, obtaining the images of the water samples can be done merely by a microscope and without the sophisticated analytical equipment. Nevertheless, the predictive power of the model in estimation of the presence of toxins in the water sample may be decreased in cases that the toxin biosynthetic clusters are silent (false positive) or a single strain of Cyanobacteria in a water sample may produce a threshold passing concentration of toxins (false negative).

We encountered challenges in the computational modeling phase due to the lack of an extensive training set and the size of the images. In order to increase the accuracy of classifying different cyanobacterial genera in the future, patch-based cropping of images can be used for the modeling section. Dividing images into several distinct patches leads models to have less trainable parameters because the size of the models is related to the input images. Applying classification after patch cropping also caused confidence in our predictions because several decisions (related to patch counts) are made for a reference test image and decreased the probability of making mistake. Attention mechanisms have achieved great success in a number of visual tasks, including image classification as it gives different values in terms of importance to different parts of images and emphasizes a certain part.

In the TCB-DS, there are several images that the shape of cyanobacterial cells' placement together as well as the shape of each bacterial cell are important. Therefore, attention-based models can be used to emphasize the region of interest (ROI) in each class to make a better result. Besides all the mentioned points, using an appropriate pre-trained model can be useful in respect of more precise classification. For example, the base model can be trained with some immense related datasets (e.g., datasets of microscopic images) first and then fine-tuned with TCB-DS.

We believe that new water quality surveillance systems must include the real-time monitoring of cyanotoxins and in case it is not possible the offline image analysis tool proposed in this study. The proposed systems versus the chemical detection of the compounds which need high tech device of Human Resource Management System (HRMS), enable the detection of different cyanobacterial genera in water samples and determine their relative concentrations. Additionally, automated quantification of the toxigenic microorganisms in the reservoirs can be the subject of future similar studies. The future development of more advanced and accurate deep learning models can contribute to water quality screening purposes and reduce the harmful consequence of human or animal intake of cyanotoxins from drinking water resources.

Future studies may investigate different preprocessing techniques to reduce image noise and simplify and strengthen the models. Using novel models and pre-trained weights can improve the performance of the identification task. To enhance the model's performance, future work could explore patch-based cropping techniques and the integration of attention mechanisms, which have shown success in various visual tasks by emphasizing relevant regions in images. Future research should also focus on expanding the TCB-DS dataset, exploring advanced computer vision techniques for automated cell detection and segmentation, incorporating attention mechanisms, leveraging transfer learning from diverse datasets, and integrating multi-modal data to further enhance the model's performance and robustness.

## Funding

No funding was received for the study.

## Ethical approval

This article does not use any human information.

## Human participants and/or animals

There is no human/animal information in this paper.

## CRediT authorship contribution statement

**Iman Kianian:** Formal analysis, Methodology, Software, Writing – original draft. **MohammadSadeq Mottaqi:** Data curation, Writing – original draft. **Fatemeh Mohammadipناه:** Conceptualization, Formal analysis, Supervision, Writing – review & editing. **Hedieh Sajedi:** Supervision, Writing – review & editing.

## Declaration of competing interest

The authors declare that they have no known competing financial interests or personal relationships that could have appeared to influence the work reported in this paper.

## Data availability

Data will be made available on request.

## Acknowledgements

Authors are thankful to Dr. Yasaman Tavakoli for her expert comments on the selected micrographs of Cyanobacteria.

## Appendix A. Supplementary data

Supplementary data to this article can be found online at <https://doi.org/10.1016/j.jenvman.2024.121274>.

## References

- Agency, U.S.E.P., 2022. Detection Methods for Cyanotoxins. Retrieved December/21 from. <https://www.epa.gov/ground-water-and-drinking-water/detection-methods-cyanotoxins>.
- Back, S.-S., Pyo, J., Pachepsky, Y., Park, Y., Ligaray, M., Ahn, C.-Y., Kim, Y.-H., Ahn Chun, J., Hwa Cho, K., 2020. Identification and enumeration of cyanobacteria species using a deep neural network. *Ecol. Indic.* 115, 106395 <https://doi.org/10.1016/j.ecolind.2020.106395>.
- Bernard, C., Baker, P., Robinson, B., Monis, P., 2007. Application of an Image Analysis System to Enumerate and Measure Cyanobacteria.
- Bunyon, C.L., Fraser, B.T., McQuaid, A., Congalton, R.G., 2023. Using imagery collected by an unmanned aerial system to monitor cyanobacteria in New Hampshire, USA, lakes. *Rem. Sens.* 15 (11).
- Chiu, Y.-T., Chen, Y.-H., Wang, T.-S., Yen, H.-K., Lin, T.-F., 2017. A qPCR-based tool to diagnose the presence of harmful cyanobacteria and cyanotoxins in drinking water sources. *Int. J. Environ. Res. Publ. Health* 14 (5), 547. <https://www.mdpi.com/1660-4601/14/5/547>.
- Cooley, M.B., Carychao, D., Gorski, L., 2018. Optimized Co-extraction and quantification of DNA from enteric pathogens in surface water samples near produce fields in California [original research]. *Front. Microbiol.* 9 <https://doi.org/10.3389/fmicb.2018.00448>.
- Deglint, J.L., Jin, C., Chao, A., Wong, A., 2019. The feasibility of automated identification of six algae types using feed-forward neural networks and fluorescence-based spectral-morphological features. *IEEE Access* 7, 7041–7053. <https://doi.org/10.1109/ACCESS.2018.2889017>.
- Deng, J., Dong, W., Socher, R., Li, L.-J., Kai, L., Li, F.-F., 2009. ImageNet: A Large-Scale Hierarchical Image Database.
- Dosovitskiy, A., Beyer, L., Kolesnikov, A., Weissenborn, D., Zhai, X., Unterthiner, T., Dehghani, M., Minderer, M., Heigold, G., Gelly, S., 2020. An Image Is Worth 16x16 Words: Transformers for Image Recognition at Scale. *arXiv preprint arXiv:2010.11929*.

- Figueroa, J., Rivas-Villar, D., Rouco, J., Novo, J., 2024. Phytoplankton detection and recognition in freshwater digital microscopy images using deep learning object detectors. *Heliyon* 10 (3), e25367. <https://doi.org/10.1016/j.heliyon.2024.e25367>.
- Gaur, A., Pant, G., Jalal, A.S., 2022. Computer-aided cyanobacterial harmful algae blooms (CyanoHABS) studies based on fused artificial intelligence (AI) models. *Algal Res.* 67, 102842 <https://doi.org/10.1016/j.algal.2022.102842>.
- Howard, A.G., Zhu, M., Chen, B., Kalenichenko, D., Wang, W., Weyand, T., Andreetto, M., Adam, H., 2017. Mobilenets: Efficient Convolutional Neural Networks for Mobile Vision Applications arXiv preprint arXiv:1704.04861.
- Jin, C., Mesquita, M.M.F., Deglint, J.L., Emelko, M.B., Wong, A., 2018. Quantification of cyanobacterial cells via a novel imaging-driven technique with an integrated fluorescence signature. *Sci. Rep.* 8 (1), 9055. <https://doi.org/10.1038/s41598-018-27406-0>.
- Khalifa, N.E.M., Taha, M.H.N., Hassanien, A.E., Hemedan, A.A., 2019. Deep bacteria: robust deep learning data augmentation design for limited bacterial colony dataset. *Int. J. Reas. base Intell. Syst.* 11 (3), 256–264. <https://doi.org/10.1504/IJRS.2019.102610>.
- Kim, J.H., Lee, H., Byeon, S., Shin, J.-K., Lee, D.H., Jang, J., Chon, K., Park, Y., 2023. Machine learning-based early warning level prediction for cyanobacterial blooms using environmental variable selection and data resampling. *Toxics* 11 (12).
- Kraft, K., Seppälä, J., Hällfors, H., Suikkanen, S., Ylöstalo, P., Anglès, S., Kielo, S., Kuosa, H., Laakso, L., Honkanen, M., Lehtinen, S., Oja, J., Tamminen, T., 2021. First application of IFCB high-frequency imaging-in-flow cytometry to investigate bloom-forming filamentous cyanobacteria in the baltic sea. *Front. Mar. Sci.* 8, 594144 <https://doi.org/10.3389/fmars.2021.594144>.
- Liu, J., Dazzo, F.B., Glagoleva, O., Yu, B., Jain, A.K., 2001. CMEIAS: a computer-aided system for the image analysis of bacterial morphotypes in microbial communities. *Microb. Ecol.* 41 (3), 173–194. <https://doi.org/10.1007/s002480000004>.
- López, Y.P., Filho, C.F.F.C., Aguilera, L.M.R., Costa, M.G.F., 2017. Automatic classification of light field smear microscopy patches using Convolutional Neural Networks for identifying mycobacterium tuberculosis. In: 2017 CHILEAN Conference on Electrical, Electronics Engineering, Information and Communication Technologies (CHILECON).
- Lu, Y., Zhang, L., Wang, J., Bian, L., Ding, Z., Yang, C., 2024. Hyperspectral upgrade solution for biomicroscope combined with Transformer network to classify infectious bacteria. *J. Biophot. (n/a)*, e202300484 <https://doi.org/10.1002/jbio.202300484>. n/a.
- Lyon-Colbert, A., Su, S., Cude, C., 2018. A systematic literature review for evidence of Aphanizomenon flos-aquae toxicity in recreational waters and toxicity of dietary supplements: 2000–2017. *Toxins* 10 (7).
- Mehdizadeh Allaf, M., Peerhossaini, H., 2022. Cyanobacteria: model microorganisms and beyond. *Microorganisms* 10 (4). <https://doi.org/10.3390/microorganisms10040696>.
- Men, H., Wu, Y., Gao, Y., Kou, Z., Xu, Z., Yang, S., 2008. Application of Support vector machine to heterotrophic bacteria colony recognition. 2008 International Conference on Computer Science and Software Engineering 1, 830–833.
- Moreira, C., Vasconcelos, V., Antunes, A., 2022. Cyanobacterial blooms: current knowledge and new perspectives. *Earth* 3 (1), 127–135.
- Nasip, Ö.F., Zengin, K., 2018. Deep learning based bacteria classification. In: 2018 2nd International Symposium on Multidisciplinary Studies and Innovative Technologies (ISMSIT).
- Neilan, B.A., Pearson, L.A., Muenchhoff, J., Moffitt, M.C., Dittmann, E., 2013. Environmental conditions that influence toxin biosynthesis in cyanobacteria. *Environ. Microbiol.* 15 (5), 1239–1253. <https://doi.org/10.1111/j.1462-2920.2012.02729.x>, 10.1111/j.1462-2920.2012.02729.x.
- Organization, W.H., 2003. Guidelines for Safe Recreational Water Environments: Coastal and Fresh Waters, vol. 1. World Health Organization.
- Otálora, P., Guzmán, J.L., Acién, F.G., Berenguel, M., Reul, A., 2023. An artificial intelligence approach for identification of microalgae cultures. *N. Biotech.* 77, 58–67. <https://doi.org/10.1016/j.nbt.2023.07.003>.
- Paerl, H.W., Huisman, J., 2008. Blooms like it hot. *Science* 320 (5872), 57–58. <https://doi.org/10.1126/science.1155398>.
- Pardeshi, R., Deshmukh, P., 2023a. Automatic classification of Desmids using transfer learning. *J. Appl. Eng. Technol. Sci. (JAETS)* 4 (2), 885–894. <https://doi.org/10.37385/jaets.v4i2.1864>.
- Pardeshi, R., Deshmukh, P., 2023b. Efficient microalgae species identification using compact convolutional neural network. *Int. J. Recent and Innov. Trends in Comput. Commun.* 11 (7s), 8–15. <https://doi.org/10.17762/ijritcc.v11i7s.6972>.
- Park, J., Lee, H., Park, C.Y., Hasan, S., Heo, T.-Y., Lee, W.H., 2019. Algal morphological identification in watersheds for drinking water supply using neural architecture search for convolutional neural network. *Water* 11 (7), 1338. <https://www.mdpi.com/2073-4441/11/7/1338>.
- Promdaen, S., Wattuya, P., Sanevas, N., 2014. Automated microalgae image classification. *Procedia Comput. Sci.* 29, 1981–1992. <https://doi.org/10.1016/j.procs.2014.05.182>.
- Prüss-Ustün, A., Wolf, J., Bartram, J., Clasen, T., Cumming, O., Freeman, M.C., Gordon, B., Hunter, P.R., Medlicott, K., Johnston, R., 2019. Burden of disease from inadequate water, sanitation and hygiene for selected adverse health outcomes: an updated analysis with a focus on low- and middle-income countries. *Int. J. Hyg. Environ. Health* 222 (5), 765–777. <https://doi.org/10.1016/j.ijheh.2019.05.004>.
- Pyo, J., Park, L.J., Pachepsky, Y., Baek, S.-S., Kim, K., Cho, K.H., 2020. Using convolutional neural network for predicting cyanobacteria concentrations in river water. *Water Res.* 186, 116349 <https://doi.org/10.1016/j.watres.2020.116349>.
- Roy, M.A., Arnaud, J.M., Jasmin, P.M., Hamner, S., Hasan, N.A., Colwell, R.R., Ford, T. E., 2018. A metagenomic approach to evaluating surface water quality in Haiti. *Int. J. Environ. Res. Publ. Health* 15 (10).
- Safford, H.R., Bischel, H.N., 2019. Flow cytometry applications in water treatment, distribution, and reuse: a review. *Water Res.* 151, 110–133. <https://doi.org/10.1016/j.watres.2018.12.016>.
- Sandler, M., Howard, A., Zhu, M., Zhmoginov, A., Chen, L.-C., 2018. Mobilenetv2: inverted residuals and linear bottlenecks. In: *Proceedings of the IEEE Conference on Computer Vision and Pattern Recognition*.
- Shaily, T., Kala, S., 2020. Bacterial image classification using convolutional neural networks. In: 2020 IEEE 17th India Council International Conference (INDICON).
- Simonyan, K., Zisserman, A., 2014. Very Deep Convolutional Networks for Large-Scale Image Recognition arXiv preprint arXiv:1409.1556.
- Sonmez, M.E., Eczacıoglu, N., Gümü, N.E., Aslan, M.F., Sabanci, K., Aşıkutlu, B., 2022. Convolutional neural network - Support vector machine based approach for classification of cyanobacteria and chlorophyta microalgae groups. *Algal Res.* 61, 102568 <https://doi.org/10.1016/j.algal.2021.102568>.
- Svirčev, Z., Drobac, D., Tokodi, N., Mijović, B., Codd, G.A., Meriluoto, J., 2017. Toxicology of microcystins with reference to cases of human intoxications and epidemiological investigations of exposures to cyanobacteria and cyanotoxins. *Arch. Toxicol.* 91 (2), 621–650. <https://doi.org/10.1007/s00204-016-1921-6>.
- Talo, M., 2019. An Automated Deep Learning Approach for Bacterial Image Classification arXiv preprint arXiv:1912.08765.
- Tavakoli, Y., Mohammadipanah, F., Hamzeh, S., & Sedighi, A. Biodiversity of Tehran freshwater cyanobacteria and remote sensing analysis of reservoirs. *Eur. J. Phycol.*, 1–12. <https://doi.org/10.1080/09670262.2023.2261113>.
- Thakur, B., Zhou, G., Chang, J., Pu, H., Jin, B., Sui, X., Yuan, X., Yang, C.-H., Magruder, M., Chen, J., 2018. Rapid detection of single E. coli bacteria using a graphene-based field-effect transistor device. *Biosens. Bioelectron.* 110, 16–22. <https://doi.org/10.1016/j.bios.2018.03.014>.
- Vaughan, L., Zamyadi, A., Ajampur, S., Almutaram, H., Freguia, S., 2022. A review of microscopic cell imaging and neural network recognition for synergistic cyanobacteria identification and enumeration. *Anal. Sci.* 38 (2), 261–279. <https://doi.org/10.1007/s44211-021-00013-2>.
- Wahid, M.F., Ahmed, T., Habib, M.A., 2018. Classification of Microscopic Images of Bacteria Using Deep Convolutional Neural Network. In: 2018 10th International Conference on Electrical and Computer Engineering (ICECE).
- World Health, O., 2017. Guidelines for Drinking-Water Quality: Fourth Edition Incorporating First Addendum, fourth ed. World Health Organization. + 1st add ed.). <https://apps.who.int/iris/handle/10665/254637>.
- Xiaojuan, L., Cunshe, C., 2009. An improved BP neural network for wastewater bacteria recognition based on microscopic image analysis. *WSEAS Trans. Comput.* 8 (2), 237–247 numpages = 211.
- Zeng, Y., Guo, Y., Li, J., 2022. Recognition and extraction of high-resolution satellite remote sensing image buildings based on deep learning. *Neural Comput. Appl.* 34 (4), 2691–2706. <https://doi.org/10.1007/s00521-021-06027-1>.
- Zhang, M., Zhang, Y., Yu, S., Gao, Y., Dong, J., Zhu, W., Wang, X., Li, X., Li, J., Xiong, J., 2023. Two machine learning approaches for predicting cyanobacteria abundance in aquaculture ponds. *Ecotoxicol. Environ. Saf.* 258, 114944 <https://doi.org/10.1016/j.ecoenv.2023.114944>.
- Zhao, Z., Alzubaidi, L., Zhang, J., Duan, Y., Gu, Y., 2024. A comparison review of transfer learning and self-supervised learning: definitions, applications, advantages and limitations. *Expert Syst. Appl.* 242, 122807 <https://doi.org/10.1016/j.eswa.2023.122807>.
- Zieliński, B., Plichta, A., Misztal, K., Spurek, P., Brzywczy-Włoch, M., Ochońska, D., 2017. Deep learning approach to bacterial colony classification. *PLoS One* 12 (9), e0184554. <https://doi.org/10.1371/journal.pone.0184554>.